

Scaling Hidden Markov Language Models

Anonymous EMNLP submission

Abstract

The hidden Markov model (HMM) is a fundamental tool for sequence modeling that cleanly separates the hidden state from the emission structure. However, this clean separation makes HMMs difficult to fit to large datasets in modern NLP, and they have fallen out of use due to very poor performance compared to fully observed models. This work revisits the challenge of scaling HMMs to language modeling datasets, taking ideas from recent approaches to neural modeling. We propose methods for scaling HMMs to massive state spaces, while maintaining compact parameterization, effective regularization, and efficient exact inference. Experiments show that this approach leads to models that are much more accurate than previous HMMs and ngram-based methods while nearing the performance of NN models.

1 Introduction

Hidden Markov models (HMMs) are a fundamental latent-variable model for sequential data. Historically they have been used extensively in NLP for tasks such as sequence modeling (Rabiner, 1990), alignment (Vogel et al., 1996), and even, in a few cases, to language modeling (Kuhn et al., 1994; Huang, 2011). Compared to other approaches for sequence models, HMMs are naturally appealing since they fully separate out the process of sequential memory from the process of generation, while allowing for exact posterior inference.

State-of-the-art systems in NLP have moved away from utilizing latent hidden states and toward deterministic deep neural models. We take several lessons from the success of deep neural models for NLP tasks: (a) the right factorization is critically important for representation learning, e.g. a feedforward model (Bengio et al., 2003) can

have the same probabilistic structure as an n-gram model while performing significantly better; (b) overparameterization is critical for finding better local optima, e.g. overly large LSTMs (Zaremba et al., 2014) show marked improvements in performance; (c) regularization choices are necessary to find good solutions for different model parameterizations, e.g. experiments by Merity et al. (2017) outline a variety of training choices.

We revisit HMMs for language modeling, positing that competitive performance may require very large models. We develop a neural parameterization for HMMs that extends them to comparable size and structure of deep models. We combine this parameterization with a modeling constraint that allows us to utilize HMMs with large state spaces, while maintaining efficient exact inference. Finally we incorporate a variant of dropout that both improves accuracy and reduces the computational overhead by an order of magnitude during training.

Experiments employ HMMs on two language modeling datasets. We find that our HMM extension significantly outperforms past HMMs as well as n-gram models. It also performs comparably to neural counterparts with a similar number of parameters while maintaining uncertainty over the state dynamics.

2 Related Work

Several recent papers have combined HMMs with neural networks. Buys et al. (2018) develop an approach to relax HMMs, but show results that either perform poorly or require altering the probabilistic structure to look more like an RNN. Krakovna and Doshi-Velez (2016) utilize model combination with an RNN to connect both approaches in a 20 state model. We demonstrate how to scale to or-

ders of magnitude more states and show stronger performance.

Prior work has considered neural parameterization of structured generative models. For HMMs, Tran et al. (2016) demonstrate improvements in POS induction with a neural parameterization of an HMM. Other work has used neural parameterization for models, such as dependency models (Han et al., 2017), hidden semi-Markov models (Wiseman et al., 2018), and context free grammars (Kim et al., 2019). These works use latent variables with relatively small state spaces, as the goal of both was structure induction rather than language modeling.

Finally, another approach to scaling to larger state spaces is to initialize with a small state space then grow the state space via a split-merge process (Petrov et al., 2006; Huang, 2011). In particular, Huang (2011) learn an HMM for language modeling via this process. Fixed-size state spaces are significantly easier to optimize for current hardware, e.g. GPUs, we therefore leave split-merge procedures for future work.

3 Background: HMMs

We are interested in learning a distribution over observed tokens $\mathbf{x} = \langle x_1, \dots, x_T \rangle$, with each token x_t an element of the finite vocabulary \mathcal{X} . Hidden Markov models (HMMs) specify a joint distribution over observed tokens \mathbf{x} and discrete latent states $\mathbf{z} = \langle z_1, \dots, z_T \rangle$, with each z_t from finite set \mathcal{Z} . For notational convenience, we define the starting state $z_0 = \epsilon$. This yields the joint distribution

$$p(\mathbf{x}, \mathbf{z}; \theta) = \prod_{t=1}^T p(x_t | z_t) p(z_t | z_{t-1}) \quad (1)$$

The distributions are parameterized as follows

$$p(z_t | z_{t-1}) \propto e^{\psi_{z_t z_{t-1}}} \quad p(x_t | z_t) \propto e^{\phi_{x_t z_t}} \quad (2)$$

with transitions $\psi \in \mathbb{R}^{|\mathcal{Z}| \times |\mathcal{Z}|}$ and emissions $\phi \in \mathbb{R}^{|\mathcal{X}| \times |\mathcal{Z}|}$. We refer to emissions $p(x_t | z_t)$ as \mathbf{O} .

We distinguish two types of parameterizations: *scalar* and *neural*. A scalar parameterization simply uses $\theta = \{\phi, \psi\}$ to fit one model parameter for each distributional parameter ($O(|\mathcal{Z}|^2 + |\mathcal{X}||\mathcal{Z}|)$ model parameters). A neural parameterization uses θ as parameters of a neural network that generates ϕ and ψ , which allows for factorization.

In order to fit an HMM to data \mathbf{x} , we must marginalize over the latent states to obtain the like-

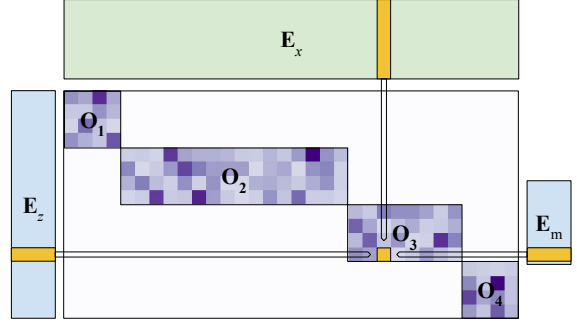


Figure 1: The emission matrix as a set of blocks $\mathbf{O}_1, \dots, \mathbf{O}_4$ (shown in transpose). Each active cell is constructed from word, state, and block embeddings.

lihood $p(\mathbf{x}) = \sum_{\mathbf{z}} p(\mathbf{x}, \mathbf{z})$. This sum can be computed in time $O(T|\mathcal{Z}|^2)$ via dynamic programming, which becomes prohibitive if the number of latent states $|\mathcal{Z}|$ is large. We can then optimize the likelihood with gradient ascent (or alternative variants of expectation maximization).

HMMs and RNNs Recurrent neural networks (RNNs) do not attempt to decouple the latent dynamics from the observed. This often leads to improved accuracy, but does not allow for posterior inference or for directly incorporating additional state information. We consider these inherently interesting properties worth exploring as alternatives. A further benefit of HMMs is that, unlike RNNs, their associative structure allows for parallel inference via the prefix-sum algorithm (Ladner and Fischer, 1980).¹

4 Scaling HMMs

Blocked Emissions Efficiency of marginal inference inherently limits the state space of general HMMs. However, we can improve inference complexity in special cases. For instance, inspired by cloned HMMs (Dedieu et al., 2019) if we know that the probability of emitting a word x_t from a state z_t is 0, i.e. $p(x_t | z_t) = 0$ then we can ignore transitions into and from that state during inference.

We enforce a stronger constraint that our HMMs have rectangular fixed-width blocked emissions,

$$\mathbf{O} = \begin{bmatrix} \mathbf{O}^1 & 0 & 0 \\ 0 & \dots & 0 \\ 0 & 0 & \mathbf{O}^M \end{bmatrix}$$

¹Quasi-RNNs (Bradbury et al., 2016) also have a logarithmic dependency on T by applying the same prefix-sum trick, but do not model uncertainty over latent dynamics.

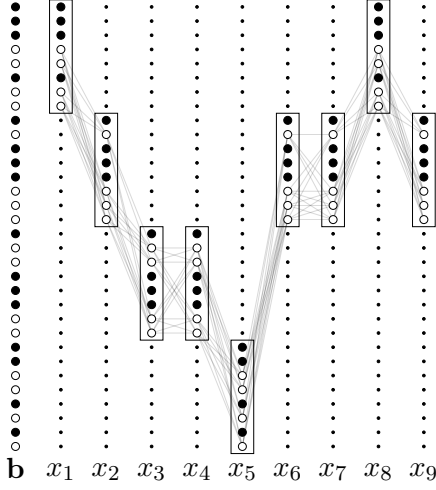


Figure 2: HMM search space with block emissions and state dropout.

where each $\mathbf{O}_m \in \mathbb{R}^{\mathcal{X}_m \times |\mathcal{Z}|/M}$ is a partition indicating which tokens \mathcal{X}_m can be emitted by states $m|\mathcal{Z}|$ through $(m+1)|\mathcal{Z}|$. Conversely let $\mathcal{Z}_x \subset \mathcal{Z}$ be the states with non-zero probability of emitting x . Exact marginalization can be computed as

$$p(\mathbf{x}) = \sum_{z_1 \in \mathcal{Z}_{x_1}} p(z_1 | z_0) p(x_1 | z_1) \times \dots \sum_{z_T \in \mathcal{Z}_{x_T}} p(z_T | z_{T-1}) p(x_T | z_T) \quad (3)$$

This gives a serial complexity of $O(T(|\mathcal{Z}|/M)^2)$

Factored Neural Parameterization Even with blocked emissions, the scalar parameterization of an HMM grows quadratically with states. We instead employ a neural parameterization. The approach is to embed each state in \mathcal{Z} ($\mathbf{E}_z \in \mathbb{R}^{|\mathcal{Z}| \times h/2}$), each token in \mathcal{X} ($\mathbf{E}_x \in \mathbb{R}^{|\mathcal{X}| \times h}$), and each block ($\mathbf{E}_m \in \mathbb{R}^{M \times h/2}$). From these we can create representations for leaving a state, entering a state, and emitting a word:

$$\mathbf{H}_{\text{out}}, \mathbf{H}_{\text{in}}, \mathbf{H}_{\text{emit}} = \text{MLP}(\mathbf{E}_m, \mathbf{E}_z)$$

The HMM distributional parameters are given by,

$$\phi = \mathbf{E}_x \mathbf{H}_{\text{emit}}^\top \quad \psi = \mathbf{H}_{\text{out}} \mathbf{H}_{\text{in}}^\top \quad (4)$$

where $\phi \in \mathbb{R}^{|\mathcal{X}| \times |\mathcal{Z}|}$ and $\psi \in \mathbb{R}^{|\mathcal{Z}| \times |\mathcal{Z}|}$. The MLP architecture follows (Kim et al., 2019). Please refer to the appendix for details. This neural parameterization takes $O(h^2 + h|\mathcal{Z}| + h|\mathcal{X}|)$ parameters (shown in Figure 1)

Algorithm 1 HMM Training

Given: block structure and model parameters
 Sample block-wise dropout mask \mathbf{b}
 Compute ϕ, ψ ignoring $b_z = 0$
for all batch examples \mathbf{x} **do**
 $\Phi = \text{LOGPOTENTIALS}(\phi, \psi, \mathbf{x}, \mathbf{b})$
 $\log p(\mathbf{x}) = \text{FORWARD}(\Phi)$
 Update embeddings $\mathbf{E}_z, \mathbf{E}_x, \mathbf{E}_\pi$

Note that parameter computation is independent of inference and can be cached completely at test-time. For training, we compute them once per batch (shown in Alg 1). For RNNs and similar models, emissions must be recomputed for each token.

Dropout as State Reduction To encourage generalization through distributed state usage, we introduce dropout to the model. We propose a form of HMM state dropout that removes states from use entirely, which has the added benefit of speeding up inference.

State dropout acts on each emission block $\mathbf{O}_1 \dots \mathbf{O}_M$ independently. Recall each block has $|\mathcal{Z}|/M$ columns. For each, we sample a binary dropout mask by sampling $\lambda \times (|\mathcal{Z}|/M)$ dropped row indices uniformly without replacement. We concatenate these to a global vector \mathbf{b} , which, along with the previous constraints, ensures,

$$p(x | z) \propto b_z 1(z \in \mathcal{Z}_x) e^{\phi_{xz}} \quad (5)$$

State dropout gives a large practical speed up for both parameter computation and inference. For $\lambda = 0.5$ we get a $4\times$ speed improvement for both, due to reduction of possible transitions. This structured dropout is also easier to exploit on GPU, since it maintains block structure with fixed-height (as shown in Figure 2).

5 Experimental Setup

Emission Blocks The model requires partitioning token types into blocks \mathcal{X}_m . While there are many partitioning methods, a natural choice is Brown clusters (Brown et al., 1992; Liang, 2005) also based on HMMs. Brown clusters are obtained by assigning every token type in \mathcal{X} a state in a HMM, then states are merged until a desired number of partitions M is reached. We construct the Brown clusters on the training portions of the datasets.

Datasets We evaluate on the Penn Treebank (Marcus et al., 1993) (929k train tokens, 10k vocab)

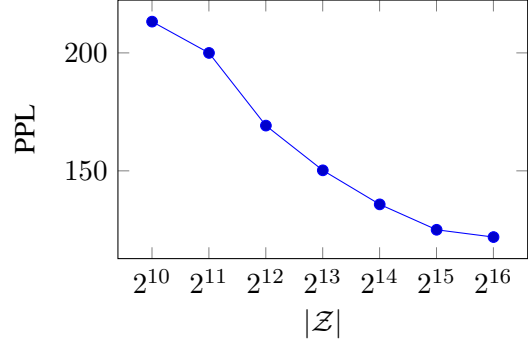
Model	Size	Val	Test
Penn Treebank			
KN 5-gram	2M	-	141.2
AWD-LSTM	24M	60.0	57.3
256 FF 5-gram	2.9M	159.9	152.0
2x256 dim LSTM	3.6M	93.6	88.8
HMM+RNN	10M	142.3	-
HMM ($ \mathcal{Z} =900$)	10M	284.6	-
VL-HMM ($ \mathcal{Z} = 2^{15}$)	7.7M	125.0	115.8
WikiText			
KN 5-gram	5.7M	248.7	234.3
AWD-LSTM	33M	68.6	65.8
256 FF 5-gram	8.8M	210.9	195.0
2x256 LSTM	9.6M	124.5	117.5
VL-HMM ($ \mathcal{Z} = 2^{15}$)	13.7M	169.0	158.2

Table 1: Perplexities on the PTB / Wikitext-2.

and wikttext2 (Merity et al., 2016) (2M train tokens, 33k vocab) datasets. For Penn Treebank we use the preprocessing from Mikolov et al. (2011), which lowercases all words and substitutes words outside of the vocabulary with unks. For Wikitext2 casing is preserved, and all words outside the vocab are replaced with the unk token. **Baselines** Baselines include AWD-LSTM (Merity et al., 2017); a 900-state scalar HMM and HMM+RNN extension, which discards the latent variable formulation (Buys et al., 2018); a KN 5-gram model (Mikolov and Zweig, 2012; Heafield et al., 2013), a 256 dimension FF model, and a 2-layer 256 dimension LSTM. We compare these models with our very large HMM (VL-HMM, $|\mathcal{Z}| = 2^{15}$) that considers 256 latent states at every timestep at test time. See the appendix for the hyperparameters for all models.

6 Results

Table 1 gives the main results. On PTB, VL-HMM is able achieve 115.8 perplexity on the test set, outperforming a strong 5-gram baseline which obtained a perplexity of 141.2 and vastly outperforming a vanilla HMM from Buys et al. (2018). The VL-HMM also outperforms the HMM+RNN extension of Buys et al. (2018). These results indicate that HMMs are a much stronger model on this benchmark than previously claimed. However, we do find that the HMM is outperformed

Figure 3: Perplexity on PTB by state size $|\mathcal{Z}|$ ($\lambda = 0.5$ and $M = 128$).

Model	Size	Train	Val	Time
VL-HMM (2^{14})	5.6M	122	136	48
- dropout	5.6M	89	145	100
- block emb	7.2M	115	134	40
- neural param	423M	119	169	14

Table 2: Ablations on PTB ($\lambda = 0.5$ and $M = 128$). Time is ms per eval batch (Run on RTX 2080).

by LSTM-based models. This trend persists in Wikitext-2, with the HMM outperforming the 5-gram model at 158.2 and 210.9 perplexity, while an LSTM achieves 117.5.

Fig. 3 examines the effect of state size. We find that performance continuously improving significantly as we grow to 2^{16} states. Table 2 considers other ablations. We find that state dropout results in both an improvement in perplexity, a large improvement in time per epoch, and a reduction in training/val performance gap. The scalar parameterization has a massive number of model parameters at 423M, compared to the neural parameterization with 5.6M parameters. Although both parameterizations reach similar training perplexity, the neural model generalizes better on validation.

7 Conclusion

This work demonstrates that scaling HMMs to large states spaces results in gains in performance. We introduced three contributions: a blocked emission constraint, a neural parameterization, and state dropout. These contributions lead to an HMM that outperforms n-gram models and prior HMMs. This work demonstrates the classical probabilistic models can scale on modern hardware and are interesting option for fitting NLP datasets.

References

- Yoshua Bengio, Réjean Ducharme, Pascal Vincent, and Christian Janvin. 2003. A neural probabilistic language model. *J. Mach. Learn. Res.*, 3(null):1137–1155.
- James Bradbury, Stephen Merity, Caiming Xiong, and Richard Socher. 2016. [Quasi-recurrent neural networks](#). *CoRR*, abs/1611.01576.
- Peter F. Brown, Peter V. deSouza, Robert L. Mercer, Vincent J. Della Pietra, and Jenifer C. Lai. 1992. Class-based n-gram models of natural language. *Comput. Linguist.*, 18(4):467–479.
- Jan Buys, Yonatan Bisk, and Yejin Choi. 2018. Bridging hmms and rnns through architectural transformations.
- Antoine Dedieu, Nishad Gothoskar, Scott Swingle, Wolfgang Lehrach, Miguel Lázaro-Gredilla, and Dileep George. 2019. [Learning higher-order sequential structure with cloned hmms](#).
- Wenjuan Han, Yong Jiang, and Kewei Tu. 2017. [Dependency grammar induction with neural lexicalization and big training data](#). In *Proceedings of the 2017 Conference on Empirical Methods in Natural Language Processing*, pages 1683–1688, Copenhagen, Denmark. Association for Computational Linguistics.
- Kenneth Heafield, Ivan Pouzyrevsky, Jonathan H. Clark, and Philipp Koehn. 2013. [Scalable modified Kneser-Ney language model estimation](#). In *Proceedings of the 51st Annual Meeting of the Association for Computational Linguistics (Volume 2: Short Papers)*, pages 690–696, Sofia, Bulgaria. Association for Computational Linguistics.
- Zhongqiang Huang. 2011. [Modeling Dependencies in Natural Languages with Latent Variables](#). Ph.D. thesis, University of Maryland.
- Yoon Kim, Chris Dyer, and Alexander M. Rush. 2019. [Compound probabilistic context-free grammars for grammar induction](#). *CoRR*, abs/1906.10225.
- Viktoriya Krakovna and Finale Doshi-Velez. 2016. [Increasing the interpretability of recurrent neural networks using hidden markov models](#).
- Thomas Kuhn, Heinrich Niemann, and Ernst Günter Schukat-Talamazzini. 1994. [Ergodic hidden markov models and polygrams for language modeling](#). pages 357–360.
- Richard E. Ladner and Michael J. Fischer. 1980. [Parallel prefix computation](#). *J. ACM*, 27(4):831–838.
- Percy Liang. 2005. Semi-supervised learning for natural language. In *MASTER’S THESIS, MIT*.
- Mitchell P. Marcus, Beatrice Santorini, and Mary Ann Marcinkiewicz. 1993. [Building a large annotated corpus of English: The Penn Treebank](#). *Computational Linguistics*, 19(2):313–330.
- Stephen Merity, Nitish Shirish Keskar, and Richard Socher. 2017. [Regularizing and optimizing LSTM language models](#). *CoRR*, abs/1708.02182.
- Stephen Merity, Caiming Xiong, James Bradbury, and Richard Socher. 2016. [Pointer sentinel mixture models](#). *CoRR*, abs/1609.07843.
- T. Mikolov and G. Zweig. 2012. Context dependent recurrent neural network language model. In *2012 IEEE Spoken Language Technology Workshop (SLT)*, pages 234–239.
- Tomas Mikolov, Anoop Deoras, Stefan Kombrink, Lukás Burget, and Jan Cernocký. 2011. [Empirical evaluation and combination of advanced language modeling techniques](#). pages 605–608.
- Slav Petrov, Leon Barrett, Romain Thibaux, and Dan Klein. 2006. [Learning accurate, compact, and interpretable tree annotation](#). page 433–440.
- Lawrence R. Rabiner. 1990. *A Tutorial on Hidden Markov Models and Selected Applications in Speech Recognition*, page 267–296. Morgan Kaufmann Publishers Inc., San Francisco, CA, USA.
- Ke M. Tran, Yonatan Bisk, Ashish Vaswani, Daniel Marcu, and Kevin Knight. 2016. [Unsupervised neural hidden markov models](#). *CoRR*, abs/1609.09007.
- Stephan Vogel, Hermann Ney, and Christoph Tillmann. 1996. [Hmm-based word alignment in statistical translation](#). In *Proceedings of the 16th Conference on Computational Linguistics - Volume 2, COLING ’96*, page 836–841, USA. Association for Computational Linguistics.
- Sam Wiseman, Stuart M. Shieber, and Alexander M. Rush. 2018. [Learning neural templates for text generation](#). *CoRR*, abs/1808.10122.
- Wojciech Zaremba, Ilya Sutskever, and Oriol Vinyals. 2014. [Recurrent neural network regularization](#). *CoRR*, abs/1409.2329.

A Appendices

A.1 Hyperparameters

For Penn Treebank and Wikitext-2, we trained the following baselines: a two layer feed-forward 5-gram model and a two layer LSTM. The feedforward model is given by the following:

$$p(w_t \mid \mathbf{w}_{<t}) = W_x \text{ReLU}(\text{Conv}(\mathbf{E}_w(\mathbf{w}_{t-4:t-1}))) \quad (6)$$

where \mathbf{E}_w gives the word embeddings and $W_x \in \mathbb{R}^{|\mathcal{X}| \times h}$ is weight-tied to the embeddings.

For the feedforward model we use a batch size of 128 and a bptt length of 64, as we found the model needed a larger batch size to train. For the LSTM, we use a batch size of 16 and a BPTT length of 32. For both baseline models we use a learning rate of 1e-3 and a dropout rate of 0.3 on the activations in the model. Both models use a hidden dimension of 256 throughout. These same hyperparameters were applied on both Penn Treebank and Wikitext-2.

For the HMMs we use a batch size of 16 and a BPTT length of 32. We use state dropout with $\lambda = 0.5$. We use a learning rate of 1e-2 for Penn Treebank, and a learning rate of 1e-3 for Wikitext-2.

All weights are initialized with the Kaiming uniform initialization.

A.2 HMM Parameterization

We use the following residual network:

$$\begin{aligned} f_i(E) &= g_i(\text{ReLU}(EW_{i1})) \\ g_i(D) &= \text{LayerNorm}(\text{ReLU}(DW_{i2}) + D) \end{aligned} \quad (7)$$

with $i \in \{\text{out}, \text{in}, \text{emit}\}$.

For the factored state embeddings in Sec. 4, we apply f to obtain

$$\begin{aligned} \mathbf{H}_{\text{out}} &= f_{\text{out}}(f_o([\mathbf{E}_m, \mathbf{E}_z])) \\ \mathbf{H}_{\text{in}} &= f_{\text{in}}(f_i([\mathbf{E}_m, \mathbf{E}_z])) \\ \mathbf{H}_{\text{emit}} &= f_{\text{emit}}(f_e([\mathbf{E}_m, \mathbf{E}_z])) \end{aligned} \quad (8)$$

A.3 Emission constraint ablation

Tbl. 3 shows the results from emission constraint ablations. For the ablations in this section, we do not use the factored state embedding and instead directly learn embeddings $\mathbf{E}_z \in \mathbb{R}^{|\mathcal{Z}| \times h}$. We examine the effect of factored state embeddings in the next section.

Constraint	$ \mathcal{Z} $	$ \mathcal{C}_x $	m	Val PPL
Brown	16384	512	32	137
Brown	16384	256	64	138
Brown	16384	128	128	134
Brown	16384	64	256	136
None	1024	-	-	180
Brown	1024	256	4	182
Brown	1024	128	8	194
Uniform	8192	128	-	150
Brown	8192	128	64	142
Uniform	16384	128	-	146
Brown	16384	128	128	136

Table 3: Emission constraint ablations on Penn Treebank.

With a VL-HMM that has $|\mathcal{Z}| = 2^{14}$ states, the model is insensitive to the number of blocks M . However, with fewer states $|\mathcal{Z}| = 2^{10}$ where we are able to use fewer blocks to examine whether the block-sparsity of the emission results in a performance loss. With $M = 4$ blocks, the block-sparse HMM matches an unconstrained HMM with the same number of states. When $M = 8$, the block-sparse model underperforms, implying there may be room for improvement with the larger HMMs that use $M > 8$ blocks.

We additionally compare the blocks induced by Brown clustering with a uniform constraint that samples subsets of states of size n independently and uniformly from \mathcal{Z} . This does not admit a partitioning, which makes it difficult to apply state dropout. We therefore zero out half of the logits of the transition matrix randomly before normalization. In the bottom of Tbl. 3, we find that models with uniform constraints are consistently outperformed by models with Brown cluster constraints as measured by validation perplexity. The models with uniform constraints also had poor validation performance despite better training performance, a symptom of overfitting.

These ablations demonstrate that the constraints based on Brown clusters used in this work may not be optimal, motivating future work that learns sparsity structure.

A.4 Factored state embedding ablation

The results of the factored state ablation are in Fig. 4. We find that the performance of independent

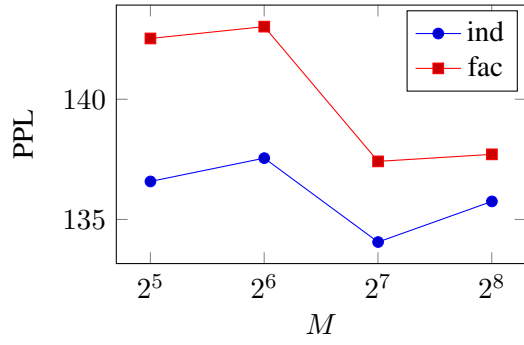


Figure 4: Perplexity on PTB by state size $|\mathcal{Z}|$ ($\lambda = 0.5$ and $M = 128$).

state embeddings with is similar to a model with factored embeddings, until the number of blocks is ≤ 64 .